

## Article

# Physical Acceptability of the Renyi, Tsallis and Sharma-Mittal Holographic Dark Energy Models in the $f(T, B)$ Gravity under Hubble's Cutoff

Salim Harun Shekh <sup>1</sup>, Pedro H. R. S. Moraes <sup>2</sup> and Pradyumn Kumar Sahoo <sup>3,\*</sup>

<sup>1</sup> Department of Mathematics, S.P.M. Science and Gilani Arts and Commerce College, Yavatmal 445301, India; da\_salim@rediff.com

<sup>2</sup> Instituto de Astronomia, Geofísica e Ciências Atmosféricas (IAG), Universidade de São Paulo (USP), São Paulo, SP 05508-090, Brazil; moraes.phrs@gmail.com

<sup>3</sup> Department of Mathematics, Birla Institute of Technology and Science-Pilani, Hyderabad Campus, Hyderabad 500078, India

\* Correspondence: pksahoo@hyderabad.bits-pilani.ac.in

**Abstract:** In the present article, we investigate the physical acceptability of the spatially homogeneous and isotropic Friedmann–Lemaître–Robertson–Walker line element filled with two fluids, with the first being pressureless matter and the second being different types of holographic dark energy. This geometric and material content is considered within the gravitational field equations of the  $f(T, B)$  (where  $T$  is the torsion scalar and the  $B$  is the boundary term) gravity in Hubble's cut-off. The cosmological parameters, such as the Equation of State (EoS) parameter, during the cosmic evolution, are calculated. The models are stable throughout the universe expansion. The region in which the model is presented is dependent on the real parameter  $\delta$  of holographic dark energies. For all  $\delta \geq 4.5$ , the models vary from  $\Lambda$ CDM era to the quintessence era.

**Keywords:** Renyi; Tsallis and Sharma–Mittle holographic dark energy models;  $f(T, B)$  gravity



**Citation:** Shekh, S.H.; Moraes, P.H.R.S.; Sahoo, P.K. Physical Acceptability of the Renyi, Tsallis and Sharma-Mittal Holographic Dark Energy Models in the  $f(T, B)$  Gravity under Hubble's Cutoff. *Universe* **2021**, *7*, 67. <https://doi.org/10.3390/universe7030067>

Academic Editors: Eugene Oks and Piero Nicolini

Received: 29 January 2021

Accepted: 10 March 2021

Published: 12 March 2021

**Publisher's Note:** MDPI stays neutral with regard to jurisdictional claims in published maps and institutional affiliations.



**Copyright:** © 2021 by the authors. Licensee MDPI, Basel, Switzerland. This article is an open access article distributed under the terms and conditions of the Creative Commons Attribution (CC BY) license (<https://creativecommons.org/licenses/by/4.0/>).

## 1. Introduction

The amazing disclosure of the increasing expansion of the universe is one of the energizing advancement areas of cosmology. This enormous change in cosmic history has been demonstrated from a differing set of high-precision observational information amassed from different cosmic sources [1–6]. The quickening paradigm is considered a result of a fascinating kind of entity, named *dark energy*.

Dark energy might anticipate the final eventual fate of the universe; its striking highlights are, as yet, unknown. To investigate such an astounding idea, various methodologies have been introduced. Among the different dynamical dark energy models, the essential applicant is the cosmological constant  $\Lambda$ . However, this experiences enormous incidents and fine-tuning problems [7,8]. As a result of this, different dynamical dark energy models have been recommended, such as K-essence [9,10], phantom energy [11,12], quintessence [13], Chaplygin gas [14–16] and holographic dark energy (HDE) models [17–21].

Here, we are particularly concerned with HDE. Inspired by black hole thermodynamics [22,23], the holographic principle states that all of the information contained in a volume of space can be represented as a hologram, which corresponds with a theory regarding the boundary of that space [24]. The most successful realization of the holographic principle is the AdS/CFT correspondence, as can be observed in the seminal reference [25]. With applications in different fields of physics, e.g., nuclear physics [26] and cosmology [27], at present, it is believed that the holographic principle should be a fundamental principle of quantum gravity.

The cosmological constant problem mentioned above [7,8] may nearly be a quantum gravity issue. In this way, as the most fundamental principle of quantum gravity, the

holographic principle should play an essential role in solving it. In fact, in [17], the first HDE model was proposed, where the holographic principle applies to cosmic acceleration. Such a model of dark energy density relies on two physical quantities on the universe's boundary: the reduced Planck mass and a cosmological length scale (which can be taken as the future event horizon of the universe). It was suggested that, in the case of a system with ultraviolet cutoff, given by  $\Lambda$ , for a region of size  $L$ , the total energy should not exceed the mass of a black hole of the same size. This results in the HDE density being defined as  $\rho_\Lambda = 3C^2 M_{Pl} / L^2$ , with  $C$  being a constant,  $M_{Pl} = 1 / \sqrt{8\pi G}$  being the reduced Planck mass and  $G$  being the Newtonian gravitational constant.

Several works exist in the literature in which the eminent authors have discussed the different kinds of HDE by using the holographic principle and dimensional analysis [28–30]. Wang et al. [31] derived the general formula for the energy density of HDE and defined the HDE model's properties, in which the future event horizon is chosen as the characteristic length scale. Pourhassan et al. [32] used observational data to perform cosmography for this holographic model based on fluid/gravity duality. They also obtained the HDE from the fluid/gravity duality constraint through cosmological observations. Sharma et al. [33] calculated the EoS and the deceleration parameter of the Tsallis HDE model to understand cosmological evolution by exploring the interacting Tsallis HDE model in a non-flat universe, with an infrared cut-off as the apparent horizon. By choosing the relationship between interacting dark matter and different HDE fluid environment models, Shekh and Ghaderi [34] have developed a Hypersurface-homogeneous cosmological model of the universe with interacting dark matter and other HDE fluid environment models. It should be a function with a unit of the inverse of cosmic time by considering a constant deceleration parameter corresponding to a purely accelerating model towards  $q = -5.4$ . In early and late periods of cosmic evolution, interacting fluids such as dark matter, holographic, and Renyi HDE fluids demonstrate dominance in Hubble's and Granda–Oliveros cut-offs, respectively.

Different kinds of infrared (IR) cut-offs have been considered in HDE models, e.g., Hubble's horizon  $H^{-1}$  [35,36], event horizon [37], particle horizon [38], conformal universe age [39,40], Ricci scalar radius [41] and Granda–Oliveros cutoff  $f$  [42]. Such HDE models with different IR cutoffs can explain the ongoing situation of the increasing speed of universe expansion in agreement with present-day observational information.

Recently, several cosmological phenomena have been discussed using Renyi and Tsallis entropies, proposed in [43,44] as generalizations of the Bekenstein entropy [22]. Such generic entropy formulations can be used in different forms to approach the DE question. From these formulations, the Renyi [45], Tsallis [29] and Sharma–Mittal HDE models [46] have been proposed.

In [47], the Renyi HDE model was examined, with the IR cutoff considered as the Hubble horizon. The examination was made through analysis of the growth rate of perturbations and statefinder hierarchy. In [48], the effects of considering different IR cutoffs, such as the particle horizon, the Ricci horizon and the Granda–Oliveros cutoff in Tsallis HDE, were explored. Observational constraints of the Tsallis HDE model were obtained in [49]. The approach developed in [47] was applied to the Sharma–Mittal HDE model in [50].

To complement the evasion possibilities of the cosmological fine-tuning problem quoted in References [9–21] and their presented applications, alternative gravity theories must be mentioned. Alternative gravity theories generalize the Einstein–Hilbert action, allowing it to depend generically on the Ricci scalar  $R$  and other scalars. Some quite interesting dark energy models have been derived from such formulations, e.g., based on  $f(R)$  [51–53] and  $f(R, \mathcal{T})$  gravity theories [54–59], with  $\mathcal{T}$  being the trace of the energy-momentum tensor.

Another possibility, which has recently drawn theoretical cosmologists' attention, is teleparallel gravity [60–65]. While in the General Relativity framework, the metric contains the gravitational potentials as responsible for the curvature of space–time, in the teleparallel

framework, the gravitational fields are represented by the torsion tensor and the curvature is not important.

Particularly, in [66], the  $f(T, B)$  gravity was proposed, with  $T$  being the torsion scalar and  $B$  the boundary term. Such a formulation was shown to be quite generic in the following sense. If the function  $f(T, B)$  is assumed to be independent of the boundary term, the  $f(T)$  gravity [67,68] is retrieved. Likewise, for a particular form of the function  $f(T, B)$ , the teleparallel equivalent of  $f(R)$  gravity is obtained.

In the following, we quote some interesting references concerning applications of the  $f(T, B)$  gravity. Zubair et al. investigated the cosmic evolution in-depth in [69]. From the different functional forms of the function  $f(T, B)$ , they have reconstructed de Sitter, power-law, phantom and even standard cosmological models. Extra polarization states of gravitational waves were obtained by Capozziello et al. in [70]. Bahamonde and Capozziello adopted the Noether symmetry approach to study dynamical systems in [71], while Bahamonde et al. analyzed the thermodynamics in  $f(T, B)$  gravity in [72].

Energized by the above references, in this article, we investigate the Renyi, Tsallis and Sharma–Mittal HDE models in the  $f(T, B)$  gravity under Hubble’s cutoff.

## 2. The $f(T, B)$ Gravity Field Equations

The  $f(T, B)$  gravity action is given as follows [66]

$$S = \int e \left[ \frac{f(T, B)}{\kappa^2} + L_m \right] d^4x, \tag{1}$$

where  $e = \det(e^i_\mu)$  is the determinant of the tetrad components,  $\kappa^2 = 8\pi G$ ,  $G$  is the Newtonian gravitational constant, the speed of light  $c$  is taken as 1,  $f(T, B)$  is a function of the torsion scalar  $T$  and boundary term  $B = \frac{2}{c} \partial_\mu (e T^\mu)$ , in which  $T^\mu = T^{\mu\nu}$  and  $L_m$  is the matter action.

By varying the action given in the equation above with respect to the tetrad, the field equations are obtained as

$$2e\delta^\lambda_\nu \nabla^\mu \nabla_\mu \partial_B f - 2e\nabla^\lambda \nabla_\nu \partial_B f + eB\partial_B f \delta^\lambda_\nu + 4e(\partial_\mu \partial_B f + \partial_\mu \partial_T f) S_\nu^{\mu\lambda} + 4e^2_\nu \partial_\mu (e S_a^{\mu\lambda}) \partial_T f - 4e\partial_T f T^\sigma_{\mu\nu} S_a^{\lambda\mu} - e f \delta^\lambda_\nu = 16\pi e T_\nu^\lambda. \tag{2}$$

where  $S_\nu^{\mu\lambda} = \frac{1}{2} (K_\nu^{\mu\lambda} + \delta_\nu^\mu T_\alpha^{\lambda\alpha} - \delta_\nu^\lambda T_\alpha^{\alpha\mu})$  and  $K_\nu^{\mu\lambda} = -\frac{1}{2} (T_\nu^{\mu\lambda} + T_\nu^{\lambda\mu} - T_\nu^{\mu\nu})$ . The matter distribution is assumed to be the combination of pressureless matter and isotropic dark energy in the form

$$\mathcal{T}_{\lambda\nu} = \mathcal{T}_{\lambda\nu}^m + \mathcal{T}_{\lambda\nu}^{de}, \tag{3}$$

which are, respectively, given as

$$\mathcal{T}_{\lambda\nu}^m = \rho_m u_\lambda u_\nu, \tag{4}$$

$$\mathcal{T}_{\lambda\nu}^{(de)} = (\rho_{de} + p_{de}) u_\lambda u_\nu - p_{de} g_{\lambda\nu}, \tag{5}$$

where  $\rho_m$  is the energy density of matter, whereas  $\rho_{de}$  and  $p_{de}$  are the pressure and energy density of HDE fluid,  $u^\nu = (0, 0, 0, 1)$  with  $u^\nu u_\nu = 1$ , where  $u^\nu$  is the four-velocity vector of the fluid.

The EoS parameter is defined as

$$\omega_{de} = \frac{p_{de}}{\rho_{de}}. \tag{6}$$

After parameterizing the energy-momentum tensor of dark energy  $\mathcal{T}_{\lambda\nu}^{de}$ , it can be expressed as follows

$$\mathcal{T}_{\lambda\nu}^{(de)} = [1, -(\omega_{de})_x, -(\omega_{de})_y, -(\omega_{de})_z] \rho_{de} \tag{7}$$

where  $(\omega_{de})_x$ ,  $(\omega_{de})_y$  and  $(\omega_{de})_z$  are the directional EoS parameters on  $x, y$  and  $z$  axis, respectively.

### 3. Metric, Friedman-Like Equations and Power Law Expansion Solutions

We consider the spatially homogeneous and isotropic Friedman–Lemâitre–Robertson–Walker line-element in the form

$$ds^2 = dt^2 - a^2(t) \left[ dr^2 + r^2(d\theta^2 + \sin^2 \theta d\phi^2) \right], \tag{8}$$

where  $a$  is the scale factor of the universe,  $(t, r, \theta, \phi)$  are the comoving coordinates and we have taken a null spatial curvature ( $k = 0$ ).

The components of (2) for the line element (8) with the stress-energy tensor (3) can be written as

$$-3H^2(3\partial_B f + 2\partial_T f) + 3H\partial_B \dot{f} - 3\dot{H}\partial_B f + \frac{1}{2}f = (\rho_m + \rho_{de}), \tag{9}$$

$$-(3H^2 + \dot{H})(3\partial_B f + 2\partial_T f) - 2H\partial_T \dot{f} + \partial_B \ddot{f} + \frac{1}{2}f = -\omega_{de}\rho_{de}, \tag{10}$$

where  $H$  is the Hubble parameter and the overhead dot represents the differentiation with respect to the cosmic time.

The torsion scalar for the metric (8) is written as

$$T = -6H^2. \tag{11}$$

It is related to the Ricci scalar as

$$R = -T + B, \tag{12}$$

The boundary term for metric (8) is obtained as

$$B = -6(\dot{H} + 3H^2). \tag{13}$$

Using (12), together with (11) and (13), the Ricci scalar is found as

$$R = -6(\dot{H} + 2H^2). \tag{14}$$

Since field Equations (9) and (10) have four unknowns and are highly nonlinear, an extra condition is needed to completely solve the system. Here, we use the volumetric power law expansion as [73]

$$V(t) = a(t)^3 = \alpha t^\beta \quad \text{and} \quad H(t) = \frac{\dot{a}}{a} = \frac{\beta}{t} \tag{15}$$

where  $\alpha > 0$  and  $\beta > 0$  are both constants. For different values of  $\beta$ , different phases of the evolution of the model are predicted. For  $0 < \beta < 1$ , a decelerated phase of the universe expansion is expected, while for  $\beta > 1$ , an accelerated phase is expected.

Keeping the relation  $a = \frac{1}{1+z}$  in mind, we obtain the following time–redshift relation

$$\frac{1}{t} = (1+z)^\frac{3}{\beta}, \tag{16}$$

### 4. Physical Acceptability of the $f(T, B)$ Gravity Holographic Dark Energy Models

#### 4.1. Renyi Holographic Dark Energy Model with Hubble’s Horizon Cutoff

The energy density of Renyi HDE is characterized as follows [73]

$$\rho_{de} = \frac{3d^2}{8\pi L^2} (1 + \pi\delta L^2)^{-1}, \tag{17}$$

with  $d$  and  $\delta$  constants. Here, by considering the Hubble horizon as a candidate for the IR-cutoff, i.e.,  $L = H^{-1}$ , the Renyi HDE density from Equation (17) is

$$\rho_{de} = \frac{3d^2 H^2}{8\pi} \left(1 + \frac{\pi\delta}{H^2}\right)^{-1}. \tag{18}$$

In view of Equation (16), the expression for the Renyi HDE provided in Equation (18) becomes, in terms of the redshift,

$$\rho_{de} = \frac{d^2 \beta^4}{216\pi} \left[ \pi\delta + \frac{\beta^2}{9} (1+z)^{\frac{6}{\beta}} \right] (1+z)^{\frac{12}{\beta}}. \tag{19}$$

The behavior of Renyi HDE density with Hubble’s horizon cutoff versus redshift for an appropriate choice of constants, especially  $\delta \geq 4.5$ , appears in Figure 1.

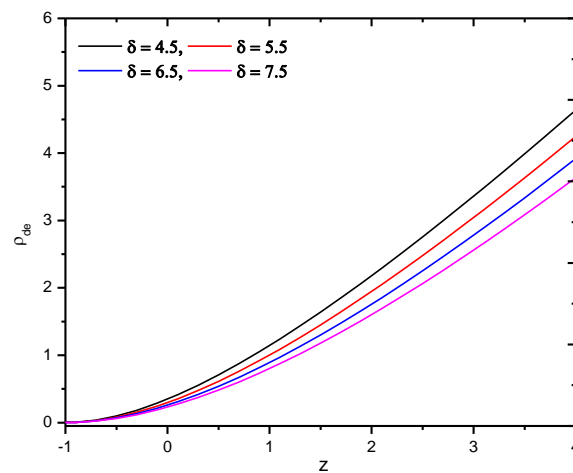


**Figure 1.** Behavior of Renyi holographic dark energy density with Hubble’s horizon cutoff versus redshift for the appropriate choice of constants  $d = 1.82$  and  $\beta = 6$ .

Using Equations (9) and (19), the energy density of pressureless matter is obtained as

$$\rho_m = \frac{(2m+1)m_1}{2} \left(\frac{-2\beta^2}{3}\right)^m (1+z)^{\frac{6m}{\beta}} + \left\{ \frac{nn_1\{(\beta-1)[2\beta(1-\beta)]^n + 2(n-1)\}}{2(\beta-1)} + \frac{n[2\beta(1-\beta)]^n}{2} \right\} (1+z)^{\frac{6n}{\beta}} - \frac{d^2 \beta^4}{216\pi} \left[ \pi\delta + \frac{\beta^2}{9} (1+z)^{\frac{6}{\beta}} \right] (1+z)^{\frac{12}{\beta}}, \tag{20}$$

with  $m, m_1, n$  and  $n_1$  being constants.

The EoS parameter of Renyi HDE is obtained as

$$\omega_{de} = - \left\{ \frac{\left\{ \frac{n(n_1+1)[2\beta(1-\beta)]^n}{2} + \frac{nn_1[1-3n+4\beta(\beta-1)(n-1)(n-2)]}{\beta(\beta-1)} \right\} (1+z)^{\frac{6n}{\beta}} + \left\{ \frac{m_1[2m(\beta-1)+\beta]}{2\beta} \left(\frac{-2\beta^2}{3}\right)^m - \frac{2mm_1(m-1)}{1} \right\} (1+z)^{\frac{6m}{\beta}}}{\frac{d^2 \beta^4}{216\pi} \left[ \pi\delta + \frac{\beta^2}{9} (1+z)^{\frac{6}{\beta}} \right] (1+z)^{\frac{12}{\beta}}} \right\}. \tag{21}$$

The behavior of the EoS parameter of Renyi HDE  $f(T, B)$  gravity model versus redshift for the appropriate choice of constants, especially for  $\delta = 7.5$ , is shown in Figure 2. It is observed that for all  $-1 \leq z \leq 0$ , the value of  $\omega_{de}$  is  $-1$ , hence it is  $\Lambda$ CDM model, and for  $0 < z$  it approaches the Quintessences region.

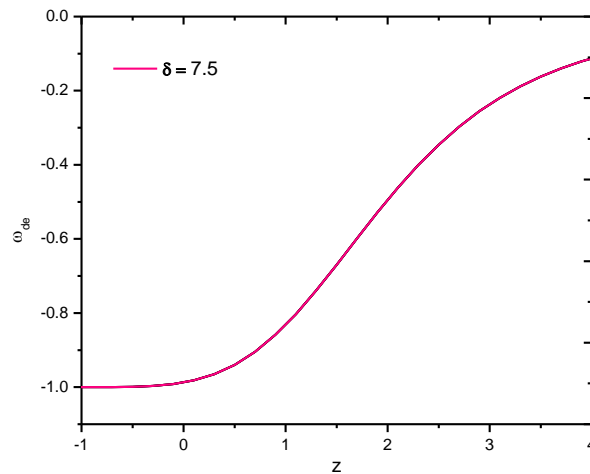


**Figure 2.** Behavior of EoS parameter of Renyi holographic dark energy density of  $f(T, B)$  gravity model in Hubble’s horizon cutoff versus redshift for the appropriate choice of constants  $d = 1.82$ ,  $\beta = 6$ ,  $m = 14$ ,  $m_1 = 0.001$ ,  $n = 10$  and  $n_1 = 7$ .

4.2. Tsallis Holographic Dark Energy Model with Hubble’s Horizon Cutoff

The energy density of Tsallis holographic dark energy is characterized as follows [73]

$$\rho_{de} = L^{2\delta-4}, \tag{22}$$

Here,  $L$  is a constant. By considering the Hubble horizon as a candidate for the IR-cutoff, i.e.,  $L = H^{-1}$ , the Tsallis HDE density from Equation (22) is

$$\rho_{de} = \frac{1}{H^{2\delta-4}} \tag{23}$$

In view of Equation (16), the expression of Tsallis HDE provided in Equation (23) becomes

$$\rho_{de} = \left(\frac{3}{\beta}\right)^{2\delta-4} (1+z)^{\frac{3(4-2\delta)}{\beta}}. \tag{24}$$

Its behavior as a function of redshift can be seen in Figure 3.

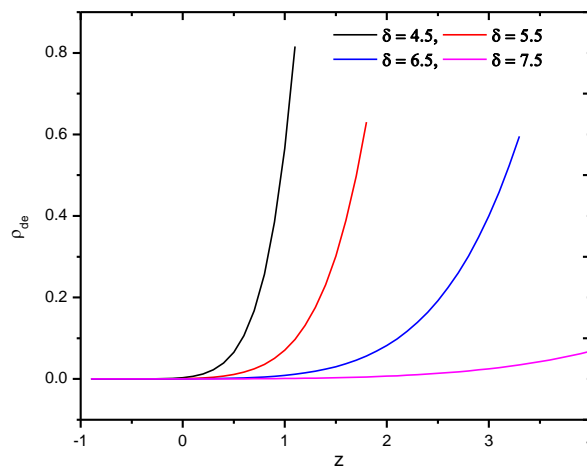


**Figure 3.** Behavior of Tsallis holographic dark energy density of  $f(T, B)$  gravity model in Hubble’s horizon cutoff versus redshift for the appropriate choice of constants  $\beta = 0.1$  and  $\beta = 6$ .

Using Equations (9) and (24), the energy density of pressureless matter is obtained as

$$\rho_m = \frac{(2m + 1)m_1}{2} \left(\frac{-2\beta^2}{3}\right)^m (1 + z)^{\frac{6m}{\beta}} + \left\{ \frac{nn_1\{(\beta - 1)[2\beta(1 - \beta)]^n + 2(n - 1)\}}{2(\beta - 1)} + \frac{n[2\beta(1 - \beta)]^n}{2} \right\} (1 + z)^{\frac{6n}{\beta}} - \left(\frac{3}{\beta}\right)^{2\delta-4} (1 + z)^{\frac{3(4-2\delta)}{\beta}}. \tag{25}$$

The EoS parameter of Tsallis HDE is obtained as

$$\omega_{de} = - \left\{ \frac{\left\{ \frac{n(n_1+1)[2\beta(1-\beta)]^n}{2} + \frac{nn_1[1-3n+4\beta(\beta-1)(n-1)(n-2)]}{\beta(\beta-1)} \right\} (1+z)^{\frac{6n}{\beta}} + \left\{ \frac{m_1[2m(\beta-1)+\beta]}{2\beta} \left(\frac{-2\beta^2}{3}\right)^m - \frac{2mm_1(m-1)}{1} \right\} (1+z)^{\frac{6m}{\beta}}}{\left(\frac{3}{\beta}\right)^{2\delta-4} (1+z)^{\frac{3(4-2\delta)}{\beta}}} \right\}. \tag{26}$$

The behavior of the EoS parameter of Tsallis HDE of  $f(T, B)$  gravity model versus redshift for the appropriate choice of constants, especially for  $\delta = 7.5$ , is clearly shown in Figure 4. It is observed that for all  $-1 \leq z \leq 0$  (here, negative redshift, i.e.,  $-1 < z < 0$ , is the blueshift which represents the present model of the universe), the value of  $\omega_{de}$  is  $-1$ , hence it is the  $\Lambda$ CDM model and further, for  $0 < z$ , it approaches the Quintessences region.

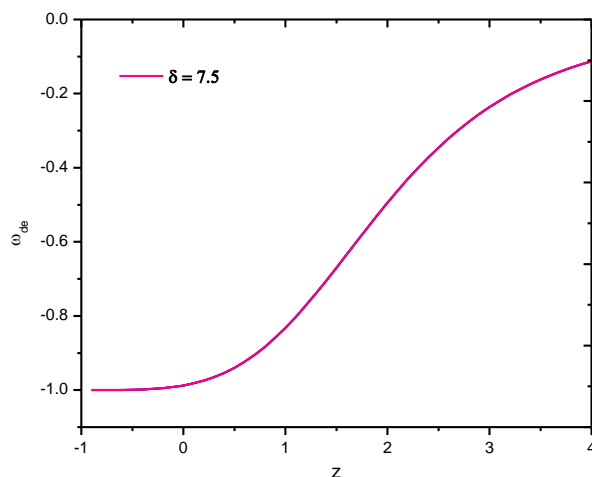


**Figure 4.** Behavior of EoS parameter of Tsallis holographic dark energy density of  $f(T, B)$  gravity model in Hubble’s horizon cutoff versus redshift for the appropriate choice of constants  $d = 1.82$ ,  $\delta = 0.1$ ,  $\beta = 6$ ,  $m = 14$ ,  $m_1 = 0.001$ ,  $n = 10$  and  $n_1 = 7$ .

4.3. Sharma–Mittal Holographic Dark Energy Model with Hubble’s Horizon Cutoff

The energy density of Sharma–Mittal HDE is characterized as follows [73]

$$\rho_{de} = \frac{3C^2 S_{SM}}{8\pi L^4}, \tag{27}$$

where  $S_{SM} = \frac{1}{d} \left[ (1 + \delta\pi L^2)^{\frac{d}{\delta}} - 1 \right]$ . Here, by considering Hubble horizon as a candidate for IR-cutoff, i.e.,  $L = H^{-1}$ , the Sharma–Mittal HDE density from Equation (27) is

$$\rho_{de} = \frac{C^2 H^4}{8\pi d} \left[ \left( 1 + \frac{\pi\delta}{H^2} \right)^{\frac{d}{\delta}} - 1 \right]. \tag{28}$$

In view of Equation (16), the expression of Sharma–Mittal HDE provided in Equation (28), becomes

$$\rho_{de} = \frac{C^2 \beta^4}{216\pi d} \left[ \left( 1 + \frac{9\pi\delta}{\beta^2(1+z)^{\frac{6}{\beta}}} \right)^{\frac{d}{\delta}} - 1 \right] (1+z)^{\frac{12}{\beta}}. \tag{29}$$

Its evolution in redshift can be seen in the figure below Figure 5.

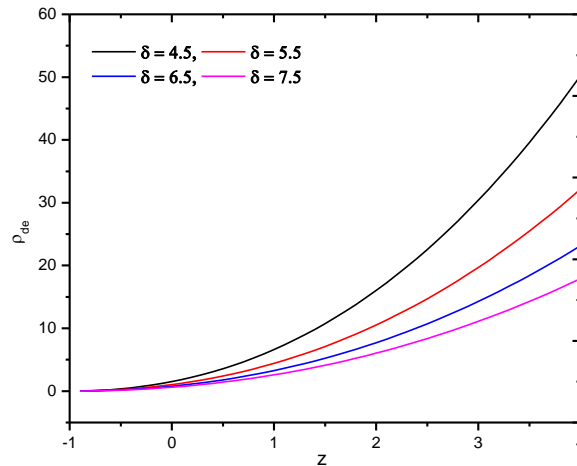


**Figure 5.** Behavior of Sharma–Mittal holographic dark energy density of  $f(T, B)$  gravity model in Hubble’s horizon cutoff versus redshift for the appropriate choice of constants  $d = 1.82$ ,  $C^2 = 0.1$ ,  $\beta = 6$ ,  $m = 14$ ,  $m_1 = 0.001$ ,  $n = 10$  and  $n_1 = 7$ .

Using Equation (9) and (29), the energy density of pressureless matter is obtained as

$$\rho_m = \frac{(2m+1)m_1}{2} \left( \frac{-2\beta^2}{3} \right)^m (1+z)^{\frac{6m}{\beta}} + \left\{ \frac{nn_1\{(\beta-1)[2\beta(1-\beta)]^n + 2(n-1)\}}{2(\beta-1)} + \frac{n[2\beta(1-\beta)]^n}{2} \right\} (1+z)^{\frac{6n}{\beta}} - \frac{C^2 \beta^4}{216\pi d} \left[ \left( 1 + \frac{9\pi\delta}{\beta^2(1+z)^{\frac{6}{\beta}}} \right)^{\frac{d}{\delta}} - 1 \right] (1+z)^{\frac{12}{\beta}}. \tag{30}$$

The EoS parameter of Sharma–Mittal HDE is obtained as

$$\omega_{de} = - \left\{ \frac{\left\{ \frac{n(n_1+1)[2\beta(1-\beta)]^n}{2} + \frac{nn_1[1-3n+4\beta(\beta-1)(n-1)(n-2)]}{\beta(\beta-1)} \right\} (1+z)^{\frac{6n}{\beta}} + \left\{ \frac{m_1[2m(\beta-1)+\beta]}{2\beta} \left( \frac{-2\beta^2}{3} \right)^m - \frac{2mm_1(m-1)}{1} \right\} (1+z)^{\frac{6m}{\beta}}}{\frac{C^2 \beta^4}{216\pi d} \left[ \left( 1 + \frac{9\pi\delta}{\beta^2(1+z)^{\frac{6}{\beta}}} \right)^{\frac{d}{\delta}} - 1 \right] (1+z)^{\frac{12}{\beta}}} \right\}. \tag{31}$$

The behavior of the EoS parameter of Sharma–Mittal holographic dark energy of  $f(T, B)$  gravity model versus redshift for the appropriate choice of constants, especially for  $\delta = 7.5$ , is shown in Figure 6 above. It is observed that for all  $-1 \leq z \leq 0$ , the value of  $\omega_{de}$  is  $-1$ , hence it is  $\Lambda$ CDM model, and further, for  $0 < z$ , it approaches the Quintessences region.

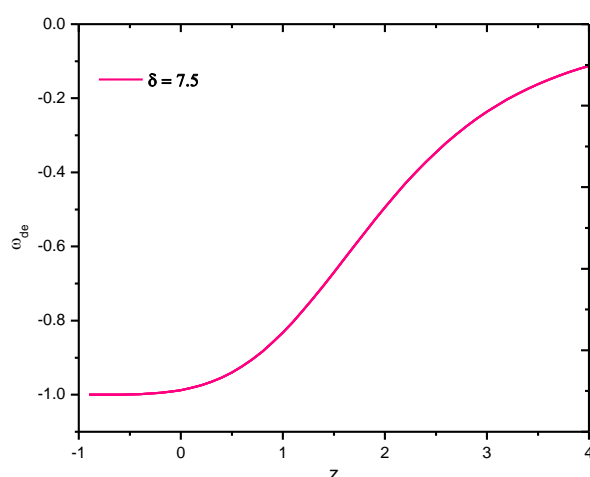


**Figure 6.** Behavior of EoS parameter of Sharma–Mittal holographic dark energy  $f(T, B)$  gravity model in Hubble’s horizon cutoff versus redshift for the appropriate choice of constants  $d = 1.82$ ,  $C^2 = 0.1$ ,  $\beta = 6$ ,  $m = 14$ ,  $m_1 = 0.001$ ,  $n = 10$  and  $n_1 = 7$ .

## 5. Discussion

The holographic principles need the degrees of freedom of a spatial region to reside not in the interior of an ordinary quantum field theory, but on the surface of the region, along with a number of degrees of freedom per unit area no greater than 1 per Planck area. Hence, the entropy of a region must not go beyond its area in Planck units [74].

The holographic principle was applied to cosmology in [74], and since then, many HDE models have appeared. In addition to those mentioned previously, see [75–81].

In the present article, we have chosen to work with HDE models in the  $f(T, B)$  theory of gravity. We have analyzed three different possibilities within this context, the Renyi, Tsallis and Sharma–Mittal HDE models, and observed that, in all possibilities for all  $-1 \leq z \leq 0$ , the value of  $\omega_{de}$  is  $-1$ , hence it is  $\Lambda$ CDM model, and further, for  $0 < z$ , it approaches the Quintessences region, which indicates the cosmic acceleration of the universe.

**Author Contributions:** S.H.S.: Writing—Original draft preparation, Investigation, Graph plotting, P.H.R.S.M.: Methodology, Formal analysis, Conceptualization, Writing, P.K.S.: Writing—Reviewing and Editing, Validation, Project administration. All authors have read and agreed to the published version of the manuscript.

**Funding:** This research received no external funding.

**Conflicts of Interest:** The authors declare no conflict of interest.

## References

1. Riess A.G.; Strolger, L.-G.; Tonry, J.; Casertano, S.; Ferguson, H.C.; Mobasher, B.; Challis, P.; Filippenko, A.V.; Jha, S.; Li, W.; et al. Type Ia Supernova Discoveries at  $z > 1$  from the Hubble Space Telescope: Evidence for past deceleration and constraints on dark energy evolution. *Astrophys. J.* **2004**, *607*, 665. [[CrossRef](#)]
2. Astier, P.; Pain, R. Observational evidence of the accelerated expansion of the universe L’acceleration de l’expansion de l’Univers du point de vue de l’observation. *Compt. Rend. Phys* **2012**, *13*, 521–538. [[CrossRef](#)]
3. Yu, H.-R.; Zhang, T.-J.; Pen, U.-L. Method for Direct Measurement of Cosmic Acceleration by 21-cm Absorption Systems. *Phys. Rev. Lett.* **2014**, *113*, 041303. [[CrossRef](#)] [[PubMed](#)]
4. Haridasu, B.S.; Luković, V.V.; D’Agostino, R.; Vittorio, N. Strong evidence for an accelerating Universe. *Astron. Astrophys.* **2017**, *600*, L1. [[CrossRef](#)]
5. Rubin, D.; Hayden, B. Is the expansion of the universe accelerating? all signs point to yes. *Astrophys. J. Lett.* **2016**, *833*, L30. [[CrossRef](#)]
6. Trentham, N. Distance measurements as a probe of cosmic acceleration. *Month. Not. Roy. Astron. Soc.* **2001**, *326*, 1328. [[CrossRef](#)]
7. Weinberg, S. The cosmological constant problem. *Rev. Mod. Phys.* **1989**, *61*, 1. [[CrossRef](#)]
8. Martin, J. The phenomenological approach to modeling the dark energy. *Compt. Rend. Phys.* **2012**, *13*, 566. [[CrossRef](#)]
9. Armendariz-Picon, C.; Mukhanov, V.; Steinhardt, Paul J. Essentials of k-essence. *Phys. Rev. D* **2001**, *63*, 103510. [[CrossRef](#)]

10. Chiba, T. Tracking K-essence. *Phys. Rev. D* **2002**, *66*, 063514. [[CrossRef](#)]
11. Caldwell, R.R.; Kamionkowski, Marc; Weinberg, Nevin N. Phantom Energy: Dark Energy with  $\omega < -1$  Causes a Cosmic Doomsday. *Phys. Rev. Lett.* **2003**, *91*, 071301. [[PubMed](#)]
12. González-Díaz, P. You need not be afraid of phantom energy. *Phys. Rev. D* **2003**, *68*, 021303. [[CrossRef](#)]
13. Zlatev, I.; Wang, L.; Steinhardt, Paul J. Quintessence, Cosmic Coincidence, and the Cosmological Constant. *Phys. Rev. Lett.* **1999**, *82*, 896. [[CrossRef](#)]
14. Amendola, L.; Finelli, F.; Burigana, C.; Carturan, D. WMAP and the generalized Chaplygin gas. *J. Cosm. Astrop. Phys.* **2003**, *7*, 005. [[CrossRef](#)]
15. Bento, M.C.; Bertolami, O.; Sen, A. A. Generalized Chaplygin gas, accelerated expansion, and dark-energy-matter unification. *Phys. Rev. D* **2002**, *66*, 043507. [[CrossRef](#)]
16. Keresztes, Z.; Gergely, L.A.; Kamenshchik, Alexander Yu.; Gorini, V.; Polarski, D. Soft singularity crossing and transformation of matter properties. *Phys. Rev. D* **2003**, *68*, 023535. [[CrossRef](#)]
17. Li, M. A Model of holographic dark energy. *Phys. Lett. B* **2004**, *603*, 1. [[CrossRef](#)]
18. Pavón, D.; Zimdahl, W. Holographic dark energy and cosmic coincidence. *Phys. Lett. B* **2005**, *628*, 206. [[CrossRef](#)]
19. Huang, Q.G.; Li, M. The holographic dark energy in a Non-flat Universe. *J. Cosm. Astrop. Phys.* **2004**, *8*, 013. [[CrossRef](#)]
20. Huang, Q.G.; Gong, Y., Supernova Constraints on a holographic dark energy model. *arXiv* **2004**, arXiv:astro-ph/0403590.
21. Gong, Y. Extended holographic dark energy. *Phys. Rev. D* **2004**, *70*, 064029. [[CrossRef](#)]
22. Bekenstein, J.D. Black holes and entropy. *Phys. Rev. D* **1973**, *7*, 2333. [[CrossRef](#)]
23. Hawking, S.W. Particle creation by black holes. *Comm. Math. Phys.* **1975**, *43*, 199. [[CrossRef](#)]
24. Hooft, G. Dimensional reduction in quantum gravity. *arXiv* **1993**, arXiv:gr-qc/9310026.
25. Maldacena, J.M. The large-N limit of super conformal field theories and super gravity. *Int. J. Theor. Phys.* **1999**, *38*, 1113. [[CrossRef](#)]
26. Liu, H.; Rajagopal, K.; Wiedemann, U. A. Wilson loops in heavy ion collisions and their calculation in AdS/CFT. *J. High Energy Phys.* **2007**, *3*, 066. [[CrossRef](#)]
27. Strominger, A. The dS/CFT correspondence. *J. High Energy Phys.* **2001**, *10*, 034. [[CrossRef](#)]
28. Jawad, A.A. Tsallis, Renyi and Sharma–Mittal holographic dark energy models in DGP brane-world. *Phys. Dark Univ.* **2019**, *26*, 100349.
29. Tavayef, M.; Sheykhi, A.; Bamba, K.; Moradpour, H. Tsallis holographic dark energy. *Phys. Lett. B* **2018**, *781*, 195. [[CrossRef](#)]
30. Aditya, Y.; Mandal, S.; Sahoo, P.K.; Reddy, D.R.K. Observational constraint on interacting Tsallis holographic dark energy in logarithmic Brans–Dicke theory. *Eur. Phys. J. C* **2019**, *79*, 1020. [[CrossRef](#)]
31. Wang, S.; Wang, Y.; Li, M. Holographic dark energy. *Phys. Rep.* **2017**, *696*, 1. [[CrossRef](#)]
32. Pourhassan, B.; Bonilla, A.; Faizal, M.; Abreu, E.M.C. Holographic dark energy from fluid/gravity duality constraint by cosmological observations. *Phys. Dark Univ.* **2018**, *20*, 41. [[CrossRef](#)]
33. Sharma, U.K.; Dubey, V.C.; Pradhan, A. Diagnosing interacting Tsallis holographic dark energy in the non-flat universe. *Int. J. Geom. Methods Mod. Phys.* **2020**, *17*, 2050032. [[CrossRef](#)]
34. Shekh, S.H.; Ghaderi, K. Hypersurface-homogeneous space–time with interacting holographic model of dark energy with Hubble’s and Granda–Oliveros IR cut-off. *Phys. Dark Univ.* **2021**, *31*, 100785. [[CrossRef](#)]
35. Xu, L. Holographic dark energy model with Hubble horizon as an IR cut-off. *J. Cosm. Astrop. Phys.* **2009**, *9*, 016. [[CrossRef](#)]
36. Liu J.; Gong, Y.; Chen, X. Dynamical behavior of the extended holographic dark energy with the Hubble horizon. *Phys. Rev. D* **2010**, *81*, 083536. [[CrossRef](#)]
37. Nomura, Y.; Remmen, G.N. Area law unification and the holographic event horizon. *J. High Ener. Phys.* **2018**, *2018*, 063 [[CrossRef](#)]
38. Sadjadi, H.M. The particle versus the future event horizon in an interacting holographic dark energy model. *J. Cosm. Astrop. Phys.* **2007**, *2*, 026. [[CrossRef](#)]
39. Huang, Z.P.; Wu, Y.L. Holographic dark energy model characterized by the conformal-age-like length. *Int. J. Mod. Phys. A* **2012**, *27*, 1250085. [[CrossRef](#)]
40. Huang, Z.P.; Wu, Y.L. Cosmological constraint and analysis on holographic dark energy model characterized by the conformal-age-like length. *Int. J. Mod. Phys. A* **2012**, *27*, 1250130. [[CrossRef](#)]
41. Li, E.K.; Zhang, Yu; Geng, Jin-Ling; Duan Peng-Fei. Generalized holographic Ricci dark energy and generalized second law of thermodynamics in Bianchi Type I universe. *Gen. Rel. Grav.* **2015**, *47*, 136. [[CrossRef](#)]
42. Khodam-Mohammadi, A.; Pasqua, A.; Malekjani, M.; Khomenko, I.; Monshizadeh, M. Statefinder diagnostic of logarithmic entropy corrected holographic dark energy with Granda–Oliveros IR cut-off. *Astrophys. Spa. Sci.* **2013**, *345*, 415. [[CrossRef](#)]
43. Renyi, A. *Probability Theory*; North-Holland: Amsterdam, The Netherlands, 1970.
44. Stallis, C. Possible generalization of Boltzmann–Gibbs entropy. *J. Stat. Phys.* **1988**, *52*, 479.
45. Moradpour, H.; Moosavi, S. A. ; Lobo, I. P. ; Morais Graça, J. P.; Jawad, A.; Salako, I. G. Thermodynamic approach to holographic dark energy and the Rényi entropy *Eur. Phys. J. C* **2018**, *78*, 829.
46. Sayahian, S.J.; Moosavi, S. A.; Moradpour, H.; Morais Graça, J. P.; Lobo, I. P.; Salako, I. G.; Jawad, A. Generalized entropy formalism and a new holographic dark energy model. *Phys. Lett. B*, **2018**, *780*, 21. [[CrossRef](#)]
47. Dubey, V.C.; Sharma, U. K.; Mamon, A. A. Interacting Rényi holographic dark energy in the Brans–Dicke theory. *Adv. High Energy Phys.* **2021**, *2021*, 6658862. [[CrossRef](#)]

48. Zadeh, M.A.; Sheykhi, A.; Moradpour, H.; Bamba, K. Note on Tsallis holographic dark energy. *Eur. Phys. J.* **2018**, *78*, 940. [[CrossRef](#)]
49. Sadri, E. Observational constraints on interacting Tsallis holographic dark energy model. *Eur. Phys. J. C* **2019**, *79*, 762. [[CrossRef](#)]
50. Sharma, U.K.; Dubey, V.C. Exploring the Sharma–Mittal holographic dark energy models with different diagnostic tools. *Eur. Phys. J. Plus* **2020**, *135*, 391. [[CrossRef](#)]
51. Amendola, L.; Polarski, D.; Tsujikawa, S. Are  $f(R)$  Dark Energy Models Cosmologically Viable? *Phys. Rev. Lett.* **2007**, *98*, 131302. [[CrossRef](#)]
52. Amendola, L.; Gannouji, R.; Polarski, D.; Tsujikawa, S. Conditions for the cosmological viability of  $f(R)$  dark energy models. *Phys. Rev. D* **2007**, *75*, 083504. [[CrossRef](#)]
53. Capozziello, S.; Cardone, V.F.; Troisi, A. Reconciling dark energy models with  $f(R)$  theories. *Phys. Rev. D* **2005**, *71*, 043503. [[CrossRef](#)]
54. Baffou, E.H.; Kpadonou, A. V. ; Rodrigues, M. E.; Houndjo, M. J. S.; Tossa, J. Cosmological viable  $f(R, T)$  dark energy model: Dynamics and stability. *Astrophys. Space Sci.* **2015**, *356*, 173. [[CrossRef](#)]
55. Houndjo, M.J.S. Reconstruction of  $f(R, T)$  gravity describing matter dominated and accelerated phases. *Int. J. Mod. Phys. D* **2012**, *21*, 1250003. [[CrossRef](#)]
56. Mishra, R. K.; Chand, A.; Pradhan, A. Dark energy models in  $f(R, T)$  theory with variable deceleration parameter. *Int. J. Theor. Phys.* **2016**, *55*, 1241. [[CrossRef](#)]
57. Amirhashchi, H.; Pradhan, A.; Jaiswal, R. Two-Fluid Dark Energy Models in Bianchi Type-III Universe with Variable Deceleration Parameter. *Int. J. Theor. Phys.* **2013**, *52*, 2735. [[CrossRef](#)]
58. Moraes, P.H.R.S.; Sahoo, P.K. The simplest non-minimal matter–geometry coupling in the  $f(R, T)$  cosmology. *Eur. Phys. J. C.* **2017**, *77*, 480. [[CrossRef](#)]
59. Sahoo, P.K.; Sahoo, P.; Bishi, B.K. Anisotropic cosmological models in  $f(R, T)$  gravity with variable deceleration parameter. *Int. J. Geom. Methods Mod. Phys.* **2017**, *14*, 1750097. [[CrossRef](#)]
60. Combi, L.; Romero, G.E. Is Teleparallel gravity really equivalent to general relativity? *Annal. Phys.* **2018**, *530*, 1700175. [[CrossRef](#)]
61. Arcos, H.I.; Pereira, J.G. Torsion gravity: A Reappraisal. *Int. J. Mod. Phys. D* **2004**, *13*, 2193. [[CrossRef](#)]
62. Maluf, J.W. The teleparallel equivalent of general relativity. *Annal. Phys.* **2013**, *525*, 339. [[CrossRef](#)]
63. Karami, K.; Abdolmaleki, A. Generalized second law of thermodynamics in  $f(T)$  gravity. *JCAP* **2012**, *04*, 007. [[CrossRef](#)]
64. Harko, T.; Francisco, F.S.L.; Otalora, G.; Saridakis, E.N.  $f(T)$  gravity and cosmology. *JCAP* **2014**, *12*, 021. [[CrossRef](#)]
65. Rezaei, T.M.; Amani, A. Stability and interacting  $f(T)$  gravity with modified Chaplygin gas. *Can. J. Phys.* **2017**, *95*, 1068. [[CrossRef](#)]
66. Bahamonde, S.; Boehmer, C. G.; Wright, M. Modified teleparallel theories of gravity. *Phys. Rev. D* **2015**, *92*, 104042. [[CrossRef](#)]
67. Cai, Y. F.; Capozziello, S.; De Laurentis, M.; Saridakis, E. N.  $f(T)$  teleparallel gravity and cosmology. *Rep. Prog. Phys.* **2016**, *79*, 106901. [[CrossRef](#)] [[PubMed](#)]
68. Li, B.; Sotiriou, T. P.; Barrow, J. D.  $f(T)$  gravity and local Lorentz invariance. *Phys. Rev. D* **2011**, *83*, 064035. [[CrossRef](#)]
69. Zubair, M.; Waheed, S.; Fayyaz, M. A.; Ahmad, I. Energy constraints and the phenomenon of cosmic evolution in the  $f(T, B)$  framework. *Eur. Phys. J. Plus* **2018**, *133*, 452. [[CrossRef](#)]
70. Capozziello, S.; Capriolo, M.; Caso, L. Weak field limit and gravitational waves in  $f(T, B)$  teleparallel gravity. *Eur. Phys. J. C* **2020**, *80*, 156. [[CrossRef](#)]
71. Bahamonde, S.; Capozziello, S. Noether symmetry approach in  $f(T, B)$  teleparallel cosmology. *Eur. Phys. J. C* **2017**, *77*, 107. [[CrossRef](#)]
72. Bahamonde, S.; Zubair, M.; Abbas, G. Thermodynamics and cosmological reconstruction in  $f(T, B)$  gravity. *Phys. Dark Univ.* **2018**, *19*, 78. [[CrossRef](#)]
73. Maity, S.; Debnath, U. Tsallis, Rényi and Sharma–Mittal holographic and new agegraphic dark energy models in D-dimensional fractal universe. *Eur. Phys. J. Plus* **2019**, *134*, 514. [[CrossRef](#)]
74. Fischler, W.; Susskind, L. Holography and Cosmology. *arXiv* **1998**, arXiv:hep-th/9806038.
75. Gao, C.; Wu, F.; Chen, X.; Shen, You-Gen. Holographic dark energy model from Ricci scalar curvature. *Phys. Rev. D* **2009**, *79*, 043511. [[CrossRef](#)]
76. Campo, S.del; Fabris, J. C.; Herrera, R.; Zimdahl, W. Holographic dark-energy models. *Phys. Rev. D* **2011**, *83*, 123006. [[CrossRef](#)]
77. Setare, M.R. Interacting holographic dark energy model in non-flat universe. *Phys. Lett. B* **2006**, *642*, 1. [[CrossRef](#)]
78. Setare, M.R.; Vagenas, E.C. The cosmological dynamics of interacting holographic dark energy model. *Int. J. Mod. Phys. D* **2009**, *18*, 147. [[CrossRef](#)]
79. Jamil, M.; Farooq, M. U.; Rashid, M. A. Generalized holographic dark energy model. *Eur. Phys. J. C* **2009**, *61*, 471. [[CrossRef](#)]
80. Ito, M. Holographic-dark-energy model with non-minimal coupling. *Europhys. Lett.* **2005**, *71*, 712. [[CrossRef](#)]
81. Myung, Y.S.; Seo, M.G. Origin of holographic dark energy models. *Phys. Lett. B* **2009**, *671*, 435. [[CrossRef](#)]